



Depósito de investigación de la Universidad de Sevilla

<https://idus.us.es/>

Esta es la versión aceptada del artículo publicado en:

This is a accepted manuscript of a paper published in:

Influence of the constructive features of RC existing buildings in their ductility and seismic performance (<https://doi.org/10.1007/s10518-020-00984-z>). Autores: Maria-Victoria Requena-Garcia-Cruz, Antonio Morales Esteban, Percy Durand Neyra, Beatriz Zapico Blanco. Revista: Bulletin of Earthquake Engineering 2021: 19 (377- 401)

DOI: <https://doi.org/10.1007/s10518-020-00984-z>

Copyright: © Springer Nature B.V. 2020

El acceso a la versión publicada del artículo puede requerir la suscripción de la revista.

Access to the published version may require subscription.

“This version of the article has been accepted for publication, after peer review (when applicable) and is subject to Springer Nature’s [AM terms of use](#), but is not the Version of Record and does not reflect post-acceptance improvements, or any corrections. The Version of Record is available online at: [http://dx.doi.org/\[insert DOI\]](http://dx.doi.org/[insert DOI])”

INFLUENCE OF THE CONSTRUCTIVE FEATURES OF RC EXISTING BUILDINGS IN THEIR DUCTILITY AND SEISMIC PERFORMANCE

Maria-Victoria Requena-Garcia-Cruz^{*a}, Antonio Morales-Esteban^{ab}, Percy Durand-Neyra^{ab}, Beatriz Zapico-Blanco^a

^aDepartment of Building Structures and Geotechnical Engineering. University of Seville. Av. Reina Mercedes, 2, 41012, Seville, Spain

^bInstituto Universitario de Arquitectura y Ciencias de la Construcción. University of Seville. Av. Reina Mercedes, 2, 41012, Seville, Spain

*corresponding author: mrequena1@us.es

Abstract

This paper aims to analyse the ductility of existing buildings to evaluate its influence in their seismic performance. This has been achieved through the retrospective analysis of an existing building in accordance with current seismic codes. This study has revealed the lack of guidance in the NCSE02 and the EC8 regarding the assessment of the ductility of existing buildings. This manuscript proposes a methodology to assess the ductility of Spanish existing buildings. For this purpose, this paper has implemented the American code procedure combined with the EC8 and the Spanish seismic code (NCSE02) requirements. A two-storey RC frame school located in the Spanish region of Huelva has been selected as a case study. Different versions of this school have been compared: as built, designed according to current best practice, EC8 provisions and NCSE02 provisions. To do so, different constructive features have been varied according to each of the ductility class requirements: geometrical properties and the reinforcement ratio of the structural elements. Nonlinear static analyses have been carried out to obtain the displacement ductility factor (μ) and the behaviour factor (q) of each model. Construction costs and the expected damage index have been determined and compared. Results have shown that the best performance, regarding the ductility and the costs, has been obtained with the models designed with deep beams. Conversely, models with wide beams, and where only the reinforcement ratios have been varied, have merely shown a slight enhancement of the resistant and ductile capacity. It has been concluded that the ductility affects the shear capacity, the seismic performance and the expected damage of RC buildings.

Keywords

Reinforced concrete buildings; nonlinear static analysis; finite element method; ductility; behaviour factor; damage level probability.

Declaration of interest

None

Nomenclature

Geometrical parameters

b cross-section overall width; subindexes “c” and “b” refer to columns and beams, respectively
b₀ dimension of the concrete core
h beam depth
 ϕ diameter; subindexes “top”, “bot” and “int” refer to the position of the beam rebar i.e. top, bottom or intermediate, respectively. The subindex “cor” refers to the longitudinal rebar in the corner of columns
s stirrups separation; subindexes “m” and “c” refer to the middle and the corner zone
 ρ reinforcement ratio; superindex “ ’ ” refers to the steel compression ratio; subindexes “cs”

Seismic action parameters

a_{gR} EC8 reference peak ground acceleration on soil type A
a_c basic ground acceleration (NCSE02)

Material parameters

σ stress; subindexes “c” and “t” refer to compression and tensile stress, respectively
 ϵ strain; subindexes “c” and “t” refer to compression and tensile strain respectively; superindexes “el” and “pl” refer to elastic and plastic strain, respectively
E₀ undamaged modulus of deformation
E_{ci} tangent modulus of deformation of concrete for zero stress

and “long” refer to the cross-section and the longitudinal reinforcement ratio for both beams and columns	K_c ratio of second stress invariants on tensile and compressive meridians
$\varepsilon_{\phi_{sy,d}}$ design steel strain at yield	Ψ dilatation angle
ω_{wd} mechanical volumetric ratio of stirrups within critical regions	f_{b0} biaxial compressive yield strength
<i>Nonlinear analysis parameters</i>	f_{c0} uniaxial compressive yield strength
μ displacement ductility factor; subindex “ ϕ ” refers to the curvature ductility factor	ϵ eccentricity of the plastic potential surface
q behaviour factor (EC8); R in American codes	ν viscosity
q_0 basic value of the behaviour factor	f_{ck} characteristic concrete compressive strength
Δ displacement; subindexes “y”, “u” and “m” refer to yield, ultimate and maximum displacements	f_{cm} concrete compressive stress strength
V basal shear force; subindexes “y”, “d”, “e”, “m” and “ly” refer to yielding, design, elastic response, maximum and first significant yield basal shear force, respectively.	f_{ct} concrete tensile stress strength
α_u/α_1 overstrength ratio (EC8)	G_{ch} crushing energy per unit area
	G_F fracture energy per unit area
	b $\varepsilon_c^{pl}/\varepsilon_c^{ch}$ ratio
	a_c/a_t dimensionless coefficient; subindexes “c”
	b_c/b_t refer to compression and “t” to tension
	l_{eq} mesh size (finite element characteristic length)
	ν poisson’s ratio
	E_s steel deformation modulus
	F_y steel yield stress

41

42

43 1. Introduction

44

45 In Spain, the vast majority of the existing reinforced concrete (RC) buildings has been constructed
 46 prior to current seismic codes. Consequently, no seismic considerations were implemented in their
 47 design procedure (Manfredi y Masi 2017). Even if considered, those requirements were not as
 48 restrictive as those in the provisions of the current code. Therefore, the seismic strengthening of
 49 these buildings has been the focus of several works over the last few years (O’Reilly y Sullivan
 50 2018). In fact, the seismic retrofitting of buildings requires a preliminary structural evaluation of
 51 their seismic performance as pointed out in Part 3 of the Eurocode-8 (EC8-3) (European Union
 52 2005).

53

54 One of the most important seismic structural parameters is ductility. Ductility considerations were
 55 first introduced in the 1960’s and 70’s as it was observed that some structures behaved better than
 56 predicted (Calvi et al. 2008). This parameter assesses the ability of a structure to undergo large
 57 deformations in the inelastic range without a substantial reduction in strength (Park 1998).
 58 Furthermore, the Eurocode-8 Part 1 (EC8-1) (European Union 2004a) establishes that it shall be
 59 verified that structures possess an adequate level of ductility.

60

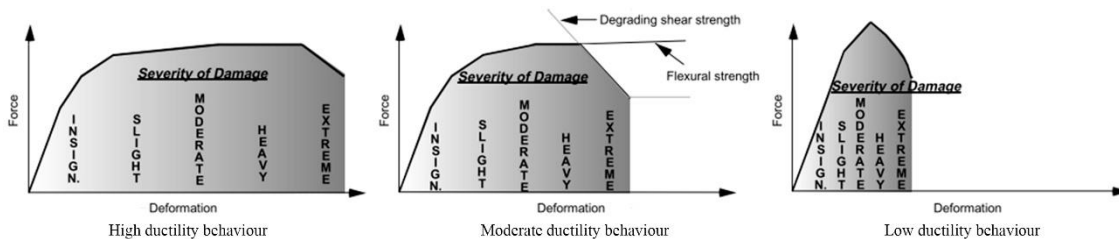
61 Ductility is a critical parameter in the seismic assessment of new and existing buildings (Alam
 62 Shahria et al. 2012). The effects of ductility are commonly considered by reducing the elastic
 63 response spectrum using a behaviour factor and performing an elastic analysis of the structure
 64 (Ferraioli et al. 2014). The behaviour factor (q in the EC8-1 and R in the American code NEHRP)
 65 depends on the structural system of the building (Kappos 1999). Thus, a correct evaluation of the
 66 behaviour factor of a structure plays a key role in the seismic safety assessment. This assumption
 67 was highlighted by the experimental results observed during past seismic events (Vona y
 68 Mastroberti 2018).

69

70 Ductility also depends on the overstrength ratio (α_u/α_1), which is defined as the ratio between the
 71 ultimate strength of a structure and its first yielding strength. The importance of overstrength has
 72 been proven by experimental and numerical research on the performance of buildings during
 73 severe earthquakes (Zahid et al. 2013). The EC8-1 states that the overstrength ratio of existing
 74 buildings must be verified.

75

76 It should be noted that most seismic evaluations of existing buildings check whether life safety is
 77 ensured, without making thorough considerations of their ductile behaviour (Alam Shahria et al.
 78 2012), while, in fact, the severity and significance of the seismic damage depends heavily on the
 79 ductility as shown in Fig. 1 (Applied Technology Council (ATC) 1998). Therefore, structural
 80 verifications should be made considering the ductility of a building in order to provide adequate
 81 retrofitting schemes (Zerbin et al. 2019).
 82



83
 84 Fig. 1. Component force-deformation behaviour, ductility, and severity of damage - FEMA 306
 85 (Applied Technology Council (ATC) 1998).
 86

87 This paper aims to analyse the ductility of existing buildings to evaluate its influence in their
 88 seismic performance. This has been achieved by means of the retrospective analysis of an existing
 89 building in accordance with current seismic codes. Different versions of a case study building
 90 have been compared: as built, designed according to current best practice, EC8 provisions and
 91 NCSE02 (Spanish Ministry of Public Works [Ministerio de Fomento de España] 2002)
 92 provisions. To do so, different constructive features (the geometrical properties and the
 93 reinforcement ratio of the structural elements) have been varied according to each of the ductility
 94 class requirements. Nonlinear static analyses have been carried out to obtain the displacement
 95 ductility factor (μ) and the behaviour factor (q) of each model. Construction costs and the expected
 96 damage index have been determined and compared.
 97

98 Finally, it should be mentioned that the works described in this paper are framed within the
 99 PERSISTAH project (*Projetos de Escolas Resilientes aos SISMos no Território do Algarve e de*
 100 *Huelva*, in Portuguese). The project is focused on the seismic retrofitting and vulnerability
 101 reduction of primary school buildings located in Algarve (Portugal) and Huelva (Spain). Schools
 102 are some of the most vulnerable buildings to earthquakes as concluded in (O'Reilly et al. 2018).
 103 In addition, the seismic hazard of the region is considerable due to the proximity of the Eurasian-
 104 African tectonic plates boundary (Amaro-Mellado et al. 2017). Moreover, it has been affected by
 105 some of the most remarkable historical earthquakes suffered in Europe, such as the 1755 Lisbon
 106 earthquake ($M_w=8.5$) and the 1969 earthquake ($M_w=8$) (Sá et al. 2018).
 107
 108

109 2. State of the art

110
 111 Research related to the ductility of buildings is of great interest and has been the focus of
 112 considerable attention over the years (Kappos 1999). Even so, the vast majority of works are
 113 based on analysing the behaviour and overstrength factors in the seismic design of new buildings
 114 (Žižmond y Dolšek 2016). These factors are quite related since the global ductility of buildings
 115 increases as the overstrength factor does (Taieb y Sofiane 2014). A major part of the studies is
 116 focused on analysing the behaviour of buildings by means of the American R -factor. It has a
 117 similar purpose as the behaviour factor introduced by the EC8-1 (Mondal et al. 2013). In (Elnashai
 118 y Mwafy 2002), a conservative overstrength value of medium and low period RC buildings of 2.0
 119 was proposed. Even the R -factor for steel moment-resisting frames was analysed in (Ferraioli et
 120 al. 2014) by means of nonlinear static and dynamic analyses. Also, the response modification
 121 factor of RC moment-resistant beams adding steel slit panels was calculated in (Zerbin et al.
 122 2019).
 123

124 Some other works are based on proposing new approaches to obtain the behaviour factor. In
125 (Costa et al. 2010), a new probabilistic methodology for the calibration of the behaviour factor
126 according to the EC8-1 procedure was presented. The authors assessed a set of regular and
127 irregular structures that comprised different RC frame structures. Considering different element
128 configurations to represent typical RC buildings is the common approach followed in these
129 studies. Also, in (Zahid et al. 2013), the authors obtained both the behaviour and overstrength
130 factors for regular and irregular buildings designated according to different European codes.
131 However, they did not vary the geometry nor the reinforcement ratio of the elements.

132
133 Likewise, some works can be found on the analysis of the ductility of buildings located in Spain.
134 In (Vielma et al. 2010), nonlinear static and dynamic analyses were carried out to estimate the
135 ductility and overstrength factors of typical RC frame typologies in Spain. In (Gómez-Martínez
136 et al. 2016a), a comparison between the seismic performance and the behaviour factor of RC
137 Spanish-code-designed wide beam and deep beam frames was carried out. Results showed that
138 wide beams had lower local ductility than deep beams. However, ductility factor results were
139 slightly higher than those established in the Spanish code for wide beams.

140
141 Few studies can be found on the analysis of the ductility of existing buildings, despite the
142 importance of such analyses. In (Vona y Mastroberti 2018), several existing RC buildings were
143 assessed to obtain their behaviour factor through a new approach. Results pointed out the lack of
144 guidance available in seismic codes to assess the behaviour factor of existing buildings.

145
146 Although nonlinear dynamic analyses have been gaining considerable interest over the past few
147 years, nonlinear static analyses provide reliable results concerning the seismic behaviour of
148 structures. In (Ferraioli et al. 2014), nonlinear static and dynamic analyses were carried out
149 concluding that realistic overstrength ratios could be obtained from pushover analyses. Moreover,
150 in (Anagnostopoulou et al. 2015), similar results concerning the inelastic response of a structure
151 were found using either static pushover or dynamic analysis. Furthermore, the EC8-1 establishes
152 that verifying the overstrength ratio values can be performed by means of nonlinear static analyses
153 (European Union 2004a).

154
155 Taking into account the ductility of buildings requires accurate analysis methods. The nonlinear
156 seismic response of existing building could be evaluated through macro-element methods.
157 Although the computational stress is reduced, these analyses are not exhaustive. Finite element
158 methods (FEM) have become a very effective tool to analyse the seismic behaviour of buildings.
159 They can provide detailed results of the structural response as well as an accurate implementation
160 of the structural element configuration. There are several works based on the use of FEM to
161 analyse the ductility of buildings. In (Reza Azadi Kakavand et al. 2018), a comparison between
162 FE models and experimental results was performed with regards to the ductility of an RC frame.
163 In (Demir et al. 2016a), numerical FE calculations were used to analyse the performance of a new
164 shear reinforcement configuration in the ductility of RC beams. The authors pointed out that
165 decreasing the spacing of stirrups would lead to insufficient bond between concrete and
166 reinforcement. In (Abou-Elfath y Elhout 2018), several RC frame configurations were defined by
167 varying the number of storeys, element dimensions, and the reinforcement ratio. FE calculations
168 were performed concluding that the R-factor is sensitive to both the number of storeys and the
169 storey height.

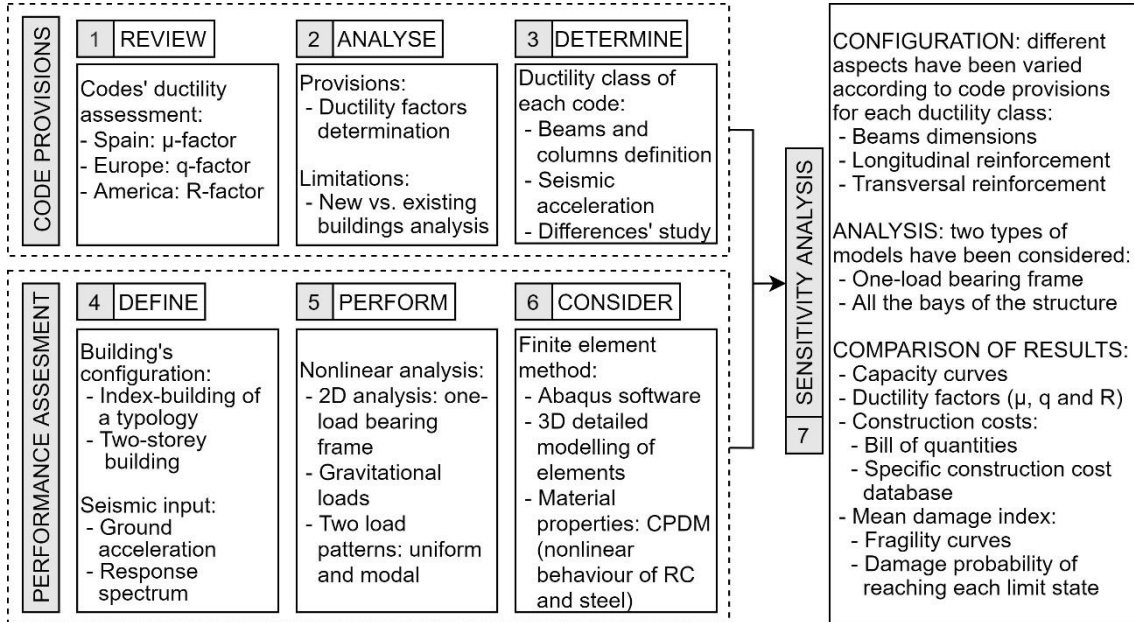
170
171 The state of the art reveals that focus has been made so far on analysing the ductility in the seismic
172 design of new buildings. Moreover, it has been found that there is a lack of guidance available in
173 seismic codes to assess the behaviour and overstrength factors of existing buildings. Therefore,
174 this paper aims to provide guidance to engineers assessing the ductility of existing structures.
175 Research on the ductility of such buildings is mainly focused on artificial models. Contrariwise,
176 in this work, the method proposed is applied to a real case-study building.

177
178

179 **3. Method**

180

181 The present section is divided into the following parts: seismic code requirements, nonlinear static
 182 analysis, finite element model technique, determination of material properties, building
 183 configuration and construction costs and damage determination. The method proposed in this
 184 study is shown in the graphical framework below (Fig. 2).
 185



186

187

Fig. 2. Graphical framework of the study.

188

189

3.1. Seismic code requirements

190

191

192

193

194

195

196

197

Clear procedures to analyse the ductility of existing buildings are hard to find due to the lack of studies (Vona y Mastroberti 2018). Regarding the ductility, the EC8 is mainly focused on new buildings. It classifies the ductility of RC buildings into three classes: low (DCL), medium (DCM) and high (DCH) dissipative capacity. The EC8 q -factor is used to reduce the elastic response spectrum in seismic design (Ferraioli et al. 2014). It is obtained according to Eq. (1) for each ductility class.

$$q = q_0 k_w \geq 1.5 \tag{1}$$

198

199

where:

200

201

q_0 is the basic behaviour factor, which depends on the structural type, the ductility class, and the overstrength ratio.

202

k_w is the factor reflecting the prevailing failure mode in structural systems with walls.

203

204

205

206

207

208

209

In this work, the building selected is characterized by a multi-storey and multi-bay frame system. For that system, the EC8 specifies an overstrength α_s/α_1 ratio of 1.30 and a k_w of 1.00. Therefore, the q -factor for DCM and DCH is 3.60 and 5.85, respectively. In the case of DCL structures, the q -factor is 1.50. Furthermore, the q -factor must be modified for irregular buildings in elevation and in plan, which is not the case.

210

211

212

213

214

In the case of existing buildings, the EC8 does not provide guidance to obtain the q -factor. However, in (Kappos 1999), a procedure related to the EC8 philosophy was proposed. The q -factor is obtained through Eq. (2), which is similar to the American R -factor definition. In this work, this procedure for obtaining q -factor has been implemented.

$$q = q_{\mu} q_{\Omega} q_{\xi} q_s \quad (2)$$

215

216 where:

217 q_{μ} is the ductility factor. Its value varies according to the period (T) of the structure to be
 218 analysed. It is used to determine the acceleration spectrum (S_a) and the displacement
 219 spectrum (S_d) of an inelastic single-degree-of-freedom system (SDOF). It is then used to
 220 obtain the target displacement of the performance point as in (Fajfar 1999).

221 q_{Ω} is the behaviour factor which depends on the effects of the overstrength (Khose et al. 2012).
 222 It depends on the material properties and the sizes and dimensions of the structural elements
 223 (Alam Shahria et al. 2012).

224 q_{ξ} is the damping-dependent factor which takes into account the effect of “added” viscous
 225 damping. It must be considered in structures with supplementary devices (Mondal et al.
 226 2013) which is not the case.

227 q_s is the redundancy factor which takes into account plastic hinge redistribution. In (Vona and
 228 Mastroberti 2018) and (Mondal et al. 2013), the authors considered a unitary value
 229 indicating correct plastic hinge distribution. This assumption has also been considered in
 230 this work.

231

232 Hence, in the case under study, the behaviour factor depends only on q_{μ} and q_{Ω} (Mwafy et al.
 233 2002).

234

235 The Spanish NCSE02 also establishes five ductility classes. However, the three main classes can
 236 be assimilated to the EC8 classification. In this work, for the sake of simplicity, the same
 237 nomenclature will be used for all of them: DCL, DCM, and DCH. In NCSE02, the classes are
 238 limited by displacement ductility factor (μ) values; i.e. 2 for DCL, 3 for DCM, and 4 for DCH.

239

240 Coherently with the above statements, both the NCSE02 and the EC8 establish different specific
 241 provisions to satisfy the appropriate ductility capacity for each class. In Tables 1 and 2, these
 242 configuration requirements are shown for beams and columns, respectively.

243

244 Table 1. Specific provisions for beams according to each seismic code and ductility classes.

	NCSE02		EC8	
	DCM	DCH	DCM	DCH
General properties			Concrete \geq C16/20 Only ribbed bars Steel class B or C	Concrete \geq C16/20 Only ribbed bars Only steel class C
Geometrical properties	$b_b \geq 200$ mm	$b_b \geq 250$ mm	$b_b \leq \min\{b_c + h_w; 2b_c\}$ $h_b / b_b \leq 3.5$ (EC2)	$b_b \geq 200$ mm $b_b \leq \min\{b_c + h_w; 2b_c\}$ $h_b / b_b \leq 3.5$ (EC2)
Reinforcement ratio	In the top: At least $2\phi 14$ mm In the bottom: At least $2\phi 14$ mm and 4% $\geq A/3$ in the ends (Being A the maximum tension rebar area at the top ends) Both in the top and bottom: $\geq A/4$ in all length (Being A the maximum negative rebar area at the ends)	In the top: $\geq A/3$ in all length (Being A the maximum negative rebar area at the ends) In the bottom: $\geq A/2$ in all length (Being A the maximum tension rebar area at the ends)	Maximum and minimum reinforcement ratio in the tension zone of beams: $\rho_{max} = \rho' + \frac{0.0018 f_{ck}}{\mu_{\phi} \varepsilon_{\phi sy, d} F_y}$ $\varepsilon_{\phi sy, d}$ is 0.2% (EHE08) $\rho_{min} = 0.5 \frac{f_{cm}}{f_{yk}}$ $\geq A/4$ in all length in both top and bottom (Being A the maximum top reinforcement at the supports)	Maximum and minimum reinforcement ratio in the tension zone of beams: $\rho_{max} = \rho' + \frac{0.0018 f_{ck}}{\mu_{\phi} \varepsilon_{\phi sy, d} F_y}$ $\rho_{min} = 0.5 \frac{f_{cm}}{f_{yk}}$
Intermediate rebar		$2\phi 10$ each 250 mm	-	-
Stirrups	$\phi \geq 6$ mm	$\phi \geq 6$ mm	$\phi_{stir} \geq 6$ mm	$\phi \geq 6$ mm

Critical region: extend 2h from column surface $s_{max} \leq \{h_b/4; 8\phi_{minlongrebar}; 150\}$ Middle region: $s_{max} \leq h_b/2$ $s_{max} \leq h_b/2$	Critical region: extend 2h from column surface $s_{max} \leq \{h_b/4; 6\phi_{minlongrebar}; 150\}$ Middle region: $s_{max} \leq h_b/2$	Critical region: first stirrup separated from beam end min 50 mm All length: $s_{max} \leq \{h_b/4; 24\phi_{stirr}; 8\phi_{minlongrebar}\}$	Critical region: first stirrup separated from beam end min 50 mm All length: $s_{max} \leq \{h_b/4; 225; 24\phi_{stirr}; 175; 6\phi_{minlongrebar}\}$
--	--	--	--

245

246

Table 2. Specific provisions for columns according to each seismic code and ductility classes.

	NCSE02		EC8	
	Mandatory if $a_c \geq 0.12g$		DCM	DCH
Geometrical properties	$b_c \geq 250$ mm			$b_c \geq 250$ mm
Reinforcement ratio			$0.01 \leq \rho \leq 0.04$ In symmetrical cross-sections: $\rho = \rho'$ Rebar maximum separation: 200mm	$0.01 \leq \rho \leq 0.04$ In symmetrical cross-sections: $\rho = \rho'$ Rebar maximum separation: 150mm
Intermediate rebar	At least, 3 rebar in each surface. $s_{max} = 200$ mm		One intermediate rebar between corner rebar	One intermediate rebar between corner rebar
Stirrups	$\phi \geq 6$ mm Middle region: $s_{max} \leq 15\phi_{stirrups}$ Critical region: extend $2b_c$ from beam surface. $s_{max} \leq \{b_c/3; 100 \text{ if } \phi_{longrebar} \leq 14; 150 \text{ if } \phi_{longrebar} \geq 16\}$ Being in this case b_c , the minor dimension of the column.		$\omega_{od} = 0.08$ at the base of columns $\phi \geq 6$ mm $s_{max} \leq \{b_0/2; 8\phi_{stirr}; 175\}$	$\omega_{od} = 0.08$ at the base and $\omega_{od} = 0.12$ above the base of columns $\phi \geq 0.4\phi_{minlongrebar} \sqrt{F_y/f_{ck}}$ $s_{max} \leq \{b_0/3; 6\phi_{stirr}; 125\}$

247

248

249

250

251

252

253

254

255

256

257

258

259

260

261

262

3.2. Nonlinear static analysis

263

264

265

266

267

268

269

270

271

272

273

274

Regarding the beam depth, both codes establish that only deep beams can be used in DCM and DCH structures. Both codes focus on the same parameters for the determination of the ductility class with different limits. In the case of the EC8, those limitations are more restrictive. Concerning the stirrups, both codes indicate similar restrictions for the spacing (using different formulae) and the diameter (≥ 6 mm) for each ductility class. The main differences can be found in the column design. In fact, the NCSE02 only indicates specific provisions for columns when the Spanish basic ground acceleration (a_c) is higher than 0.12g.

It should be noted that the minimum requirements from other structural codes may provide greater amount of reinforcement than that based on the seismic design (Žižmond y Dolšek 2016). In the case of Spain, the EHE08 (Spanish Ministry of Public Works [Ministerio de Fomento de España] 2008) concerning RC must be considered.

The aforementioned factors, which describe the dissipative capacity of buildings, can be obtained by means of nonlinear static or dynamic analyses. The state of the art revealed that no significant differences were obtained from carrying out each type of analysis for in plan and in elevation regular structures. Therefore, in this work, the seismic performance of the models has been assessed by means of nonlinear static analyses (pushover). Torsional effects can play a key role in existing asymmetric buildings. In this case, the building is symmetric, presenting a homogenous distribution of frames, bays, infills, masses and openings (Fig. 3). Therefore, torsional effects can be considered negligible as in (Vielma et al. 2010) and the structures have been modelled in 2D. In addition, FEM has been used to model the structures. This method is preferred in earthquake engineering as it provides detailed information of the damage evolution in the concrete and steel (Reza Azadi Kakavand et al. 2018).

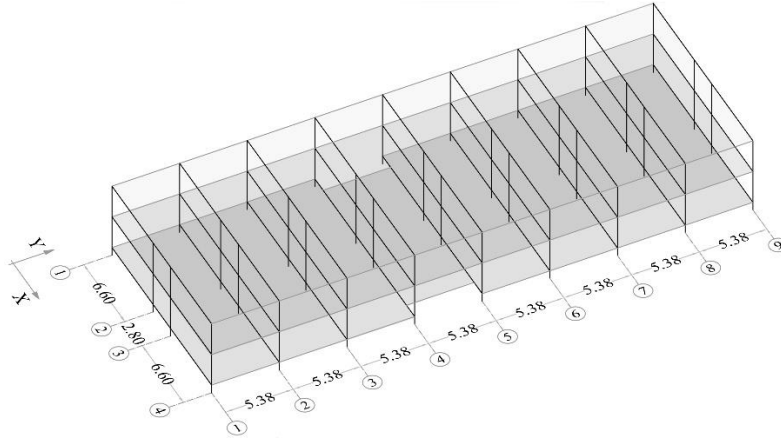


Fig. 3. 3D view of the building.

An evaluation of the q -factor of existing buildings has been undertaken by assessing the two components contributing to it (Mwafy et al. 2002): ductility and overstrength factors. These factors are based on the nonlinear behaviour of the building and the bilinearization of its capacity curve (Fig. 4). Several approaches can be found to estimate the bilinear curve as analysed by (Park 1998). In this study, the bilinear curve has been obtained according to the N2-method (Fajfar 2000). This method is based on the equivalent elasto-plastic energy absorption. Moreover, this method is settled in Annex B of the EC8-1 and it is later used to determine the performance point of the building.

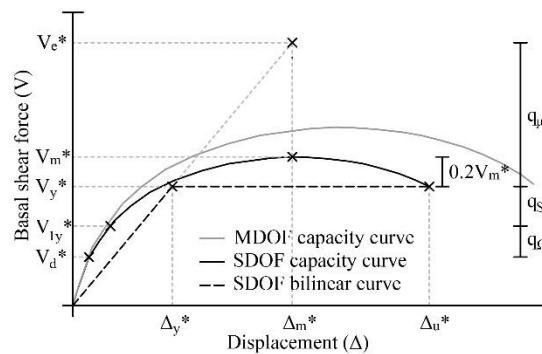


Fig. 4. Determination of the idealized elasto-perfectly plastic force-displacement relationship (EC8-1).

Where SDOF refers to the single degree of freedom system and MDOF refers to the multi degree of freedom system. Variables followed by * concern the SDOF system.

The first approach proposed for the assessment of the ductility factor was (Miranda y Bertero 1994). Since then, several approaches have been developed. However, (Miranda y Bertero 1994) remains the most used and has been widely accepted. The authors proposed the expressions Eq. (3) and (4) depending on the transition period (T_0) value of the building (Fajfar 1999). Eq. (4) is assumed for structures that exhibit a period higher than 0.5 seconds (Mwafy et al. 2002). In this work, Eq. (3) was used due to the value of the period of the models analysed.

$$q_{\mu} = \sqrt{2\mu - 1} \quad T \leq T_0 \quad (3)$$

$$q_{\mu} = \mu \quad T \geq T_0 \quad (4)$$

The displacement ductility factor was first defined in (Park 1998). It represents the ratio between the ultimate displacement and the yield displacement as expressed in Eq. (5). The overstrength factor represents the ratio between the yielding base shear and the design base shear as shown in Eq. (6) (Park 1998). This ratio is expressed as α_u/α_1 in the EC8. α_u represents the ultimate strength

306 of the structure before collapse while α_1 is the force for the first plastic hinge is formed in any
307 member (European Union 2004a).
308

$$\mu = \frac{\Delta u}{\Delta y} \quad (5)$$

$$q_{\Omega} = \frac{V_y}{V_d} = \frac{\alpha_u}{\alpha_1} \quad (6)$$

309

310

311 **3.3. Finite element model technique**

312

313 In this study, the FE numerical simulations have been performed through the ABAQUS software
314 (Dassault Simulia 2014a), which is a general-purpose FE program (Demir et al. 2016b). Models
315 have been composed of 3D-solid concrete elements combined with 1D-truss steel rebar elements.
316 Tie constraints have been determined to bond the concrete parts: columns to columns and beams
317 to columns. The “embedded region” constraint has been determined to fully bond the steel rebars
318 and the concrete parts (Alfarah et al. 2017). “Encastré” type boundary conditions have been
319 determined in each column base. Meshing has been performed for each element part. It should be
320 pointed out that the element type must be properly selected for each element during meshing.

321

322 Two steps have been generated to obtain the pushover curve in ABAQUS. First, a “Static,
323 General” step in which the gravitational loads have been added. Then, a second “Static, Riks”
324 step, in which the horizontal loads have been applied. The “Riks” method has been generally used
325 to predict the unstable geometrically nonlinear collapse of a structure (Dassault Simulia 2014b).
326 This method assumes that all load magnitudes vary with a single scalar parameter and no
327 bifurcations occur during the analysis (Fu 2009). All applied loads have been designed as
328 “concentrated” at beams nodes. These are the only load type permitted in the “Riks” step as well
329 as “Body” type forces. EC8 establishes that two load patterns must be taken into account in
330 nonlinear static analyses: one proportional to the product of the masses and the height of the
331 storeys and one proportional to the first vibration mode displacements. In this case, the first one
332 has been considered since similar capacity curves were obtained for each pattern as in (Requena-
333 García-Cruz et al. 2019). Finally, the reaction forces (RF in Abaqus) have been obtained from the
334 sum of each node force at the column bases and for the direction of interest. Then, the
335 displacements (U in Abaqus) of the control node have been determined.

336

337 **3.4. Determination of material properties.**

338

339 There are several approaches to represent the nonlinear response of concrete i.e. plasticity and
340 damage theories (Alfarah et al. 2017). The vast majority of works on concrete implemented these
341 theories to simulate its nonlinear behaviour (Tao y Chen 2015). It should be noted that the
342 concrete response in compression acts primarily according to the plasticity theory and in tension,
343 it is attributed to the damage (Lubliner et al. 1989). Therefore, a new model named concrete
344 plastic damage model (CPDM) was presented to consider both plasticity and damage theories
345 (Dassault Simulia 2014b) and the inelastic behaviour of RC (Demir et al. 2016b). In this paper,
346 the concrete was modelled according to the CPDM proposed by (Alfarah et al. 2017). This model
347 was based on the formulation developed by (Lubliner et al. 1989) and (Lee y Fenves 1998), which
348 is implemented in the ABAQUS CPDM input. Moreover, CPDM does not require calibration nor
349 validation with experimental results and uses laws based on European recommendations.

350

351 The concrete behaviour depends on five constitutive parameters that are given in Table 3 and are
352 commonly used in CPDM analyses as in (Demir et al. 2016b). The material parameters for the
353 simulation of the concrete are tabulated in Table 4. The RC is designated as HA-175 and the steel
354 rebar as AEH-400, in accordance with the existing documentation of the school analysed. These
355 terms refer to the designation of the structural materials of old Spanish RC codes. The Poisson

356 coefficient may be taken as 0.2 according to Eurocode-2 (EC2) (European Union 2004b). The
 357 material properties of the reinforcement steel are E_s 200,000 MPa, F_y 420 MPa and ν 0.3.
 358

359 Table 3. Parameters of CPDM.

K_c	Ψ ($^\circ$)	f_{b0}/f_{c0}	ϵ	ν
0.7	13	1.16	0.1	0.0001

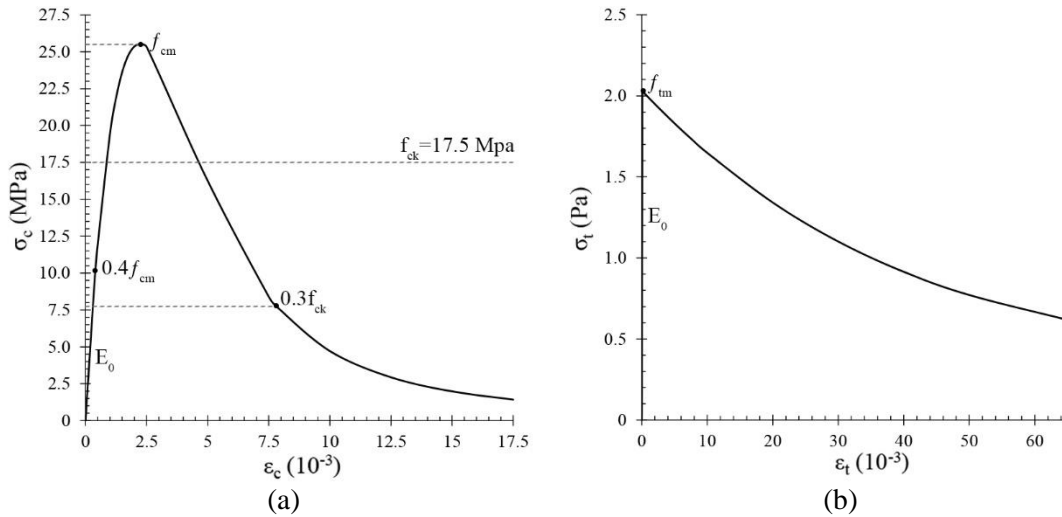
360

361 Table 4. Parameters for the simulation of the concrete.

f_{ck} (MPa)	f_{cm} (MPa)	f_{ct} (MPa)	E_0 (MPa)	E_{ci} (MPa)	G_{ch} (N/mm)	G_F (N/mm)	b	a_c	a_t	l_{eq} (mm)	b_c	b_t
17.5	25.5	2.03	25,252.88	29,9433.82	20.57	0.13	0.8	7.87	1	125	305.22	2918.77

362

363 The stress/strain relation of uniaxial compressive and tensile behaviour of concrete are depicted
 364 in Fig. 5(a) and Fig. 5(b), respectively. These plots and the compressive/tensile damage laws
 365 (damage evolution) constitute the required input of any model to describe the global structural
 366 behaviour of RC (Alfarah et al. 2017). It should be noted that only the inelastic strain must be
 367 implemented in ABAQUS. It is calculated as the strain minus the elastic strain. The failure of the
 368 concrete is established as $0.3f_{ck}$ (Grassl et al. 2013).
 369



370

371

372 Fig. 5. Stress-strain relation of uniaxial compressive (σ_c - ϵ_c) (a) and tensile (σ_t - ϵ_t) (b) behaviour of
 373 concrete.

374

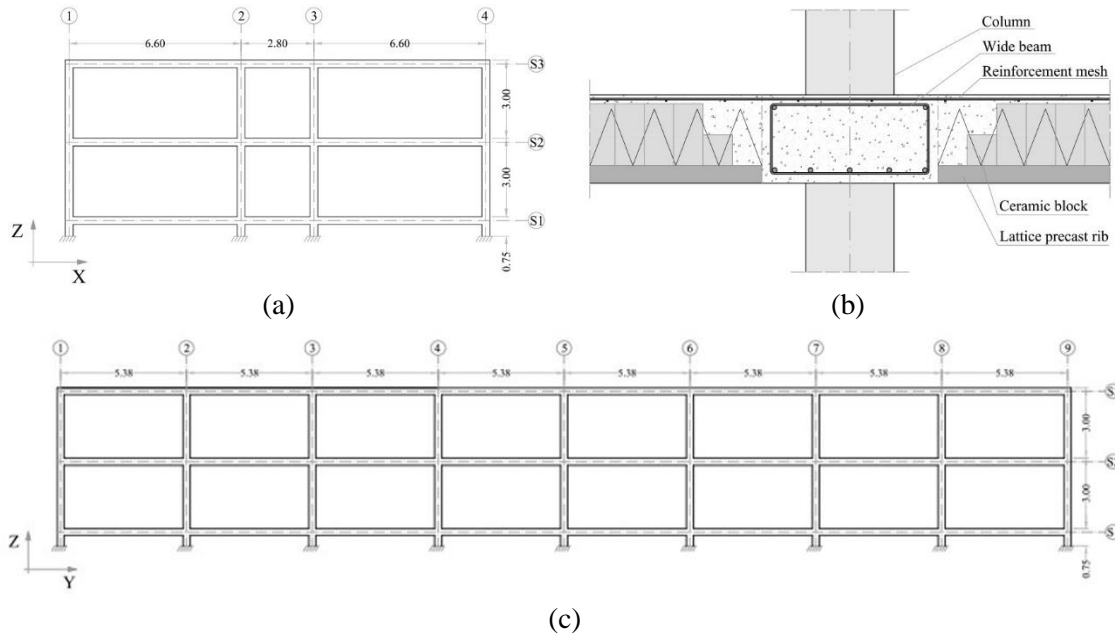
375 In addition, a sensitivity analysis on the variability of the material properties has been performed,
 376 considering a +/-10% variation of f_{ck} , E_0 , E_s and F_y
 377

378

3.5. Building configuration

379

380 In Huelva, a total amount of 138 primary school buildings has been identified, 60% of which are
 381 two-storey RC frame buildings. Most of them were constructed during the 1970's leading to a
 382 lack of seismic considerations in their design, such as the use of RC wide-beams frames or short
 383 columns. These elements are known to be some of the main causes of building damage during
 384 earthquakes (Rodgers 2012). It should be noted that the NCSE94 (first Spanish seismic code)
 385 (Spanish Ministry of Public Works [Ministerio de Fomento de España] 1994) was introduced in
 386 1994. In addition, these buildings share similar constructive characteristics: structural element
 387 sizes, height and bay dimensions. For these reasons, this type of building has been selected as the
 388 most relevant for this study. One of these buildings has been designated as the index building for
 389 the typology due to the amount and quality of available blueprints and documentation. It is a two-
 390 storey building composed of RC frames and of 30 cm thickness ribbed slabs, spanning in the Y
 391 direction. The views of the building, which are representative of the rest of the buildings of this
 392 typology, are shown in Fig. 6.



398 Fig. 6. School configuration: load bearing (a) and tie (c) frames geometry; and wide beam cross-
 399 section and ribbed slab configuration (b).

401 The building is located in Almonte, (Huelva), where a PGA value of 0.1g is determined according
 402 to the Spanish updated seismic action values (Spanish Ministry of Public Works [Ministerio de
 403 Fomento de España] 2012). The elastic response spectrum considered has been taken from the
 404 EC8 provisions. The PGA designated must be multiplied by 0.8 to obtain the EC8 reference
 405 ground acceleration (a_{gR}) as indicated by the Spanish EC8 National Annex (Spanish Ministry of
 406 Public Works [Ministerio de Fomento de España] 1998). This value is then multiplied by the
 407 importance factor (γ_I) to determine the design ground acceleration (a_g) according to EC8. School
 408 important class is III, resulting in a γ_I -factor of 1.30 (Spanish Ministry of Public Works [Ministerio
 409 de Fomento de España] 1998). According to a nearby geotechnical study, the soil is characterized
 410 by the presence of medium-low compactness silt-sand corresponding to a type C soil of EC8.

412 Additional gravitational loads (GL) to the self-weight (W) of the structural elements have been
 413 calculated using Eq. (7), according to the NCSE02 -dead loads (DL) and live load (Q)-.

$$GL = W + DL + 0.3Q \quad (7)$$

416 where:

417 DL are the sum of the weight of ribbed slabs, internal partitions, the ceiling and the ceramic
 418 flooring which is 5.5 kPa

419 Q is the correspondent value for public spaces according to the Spanish CTE-DB-SE-AE
 420 (Spanish Ministry of Public Works [Ministerio de Fomento de España] 2009), which is 3
 421 kPa.

423 3.6. Versions of the case study building compared

425 Several configurations of the load-bearing frame (X-direction) have been analysed in order to
 426 determine the variability of the ductility value. The length of the bays has remained unchanged,
 427 while several combinations of the structural element dimensions and reinforcement ratios have
 428 been selected, reproducing typical RC school configurations. Models have been determined
 429 according to the EC8 and the NCSE02 specific provisions to comply with each ductility class.
 430 According to the codes, both the cross-section and the longitudinal reinforcement ratios for the
 431 DCM and DCH classes are similar. The NCSE02 does not provide specific provisions for columns

432 since the a_c in Almonte is less than 0.12g. Therefore, only models designed according to EC8
 433 have been considered in the analyses.

434

435 All models have been first analysed to comply with the stresses derived from GL . In fact, the
 436 EHE08 requirements for the minimum reinforcement ratio have been considered. Table 5 shows
 437 the geometrical properties of the structural elements and their reinforcement detailing of each of
 438 the models to be assessed.

439

440 Table 5. Geometric properties of each model to be assessed.

Models	Beams												Columns												
	b	h	n_{top}°	ϕ_{top}	n_{bot}°	ϕ_{bot}	n_{int}°	ϕ_{int}	ϕ_{stir}	s_c	s_m	ρ_{cs}	ρ_{long}	h	b	n_{cor}°	ϕ_{cor}	n_{int}°	ϕ_{int}	ϕ_{stir}	s_c	s_m	ρ_{cs}	ρ_{long}	
Real	600	300	3	10	6	20		6	255	255	1.18	2.07	300	300	4	12		6	263	263	0.50	2.07			
RealMo	300	600	3	10	6	20		6	255	255	1.18	2.07	300	300	4	12		6	263	263	0.50	2.07			
M1	300	400	3	16	6	20	2	10	6	100	250	2.07	2.62	300	300	4	12	4	10	6	95	195	0.85	3.45	
H1	600	400	2	14	6	16	2	14	6	95	202	0.63	3.22	300	300	4	12	4	12	6	95	213	1.00	3.63	
M2	600	300	3	10	6	20	2	10	6	75	250	1.18	2.74	300	300	4	12	4	10	6	95	195	0.85	3.46	
H2	600	300	3	14	6	20	2	14	6	75	202	1.30	3.19	300	300	4	12	4	12	6	95	159	1.00	3.77	
S8	600	300	3	10	6	20		8	150	255	1.18	2.81	300	300	4	12		8	150	263	0.50	2.81			
S6_4LE	600	300	4	10	6	20		6	150	255	1.22	4.14	300	300	4	12		6	150	263	0.50	4.14			
Supduct	600	300	3	10	6	20		6	50	150	1.18	4.30	300	300	4	12	4	12	6	50	150	1.00	5.88		

441

442 To summarize, three different constructive features have been varied: the beam dimensions, the
 443 longitudinal reinforcement, and the transversal reinforcement, resulting in nine models:

- 444 – In the “Real” model, no changes have been applied: it has been designed with the same
 445 element dimensions and reinforcement ratios as the existing building.
- 446 – In the “RealMo” model, only the orientation of the beams has been changed, transforming
 447 the wide beams into deep beams.
- 448 – In the “M1” and “H1” models, the three aspects have been changed according to the DCM
 449 and DCH EC8 ductility classes, respectively.
- 450 – For the models “H2” and “M2”, the same applies, but only the reinforcement ratios have
 451 been modified while the beam sizes have not been changed.
- 452 – In the “S” models, only the transversal reinforcement ratio varies since it is mainly used
 453 to resist the shear stress produced by earthquakes. In “S8”, the diameter of the stirrups
 454 has been increased to 8mm. In “S6_4LE”, four legged stirrups of 6mm diameter have
 455 been used.
- 456 – The “Supduct” model has been designed with minimum separation of the stirrups and the
 457 longitudinal rebar, with the beam dimensions unchanged.

458

459 First, a pushover analysis has been carried out on one load-bearing frame (Fig. 6 (a)) of each of
 460 the nine models. The goal of this analysis is to obtain the relative influence of each aspect in the
 461 ductility value.

462

463 Considering the results of this phase, the most relevant models have been analysed by means of
 464 a similar pushover analysis, this time considering all the bays of the structure; i.e. the complete
 465 building. These models were the “Real” and “RealMo” and have been analysed in order to
 466 determine the global behaviour of the structures.

467

468

469 3.7. Construction costs and damage level determination

470

471 In this work, the construction costs (C) of each model have been determined. The costs have been
 472 estimated by means of a bill of quantities. Unlike the rest of studies of this type, a specific detail
 473 of the prices and the dimensions of each model has been performed. To do so, an updated Spanish
 474 construction cost database has been used (CYPE Ingenieros S.A.). This database contains the
 475 costs of the materials and the work units, taking into account the labour and indirect costs, the
 476 industrial benefit and the construction times.

477

The specific detail of the prices considering the characteristics of each of the models analysed are listed in Table 6. The volume of concrete and the weight of steel of each of the models has been measured and multiplied by the cubic meter price calculated considering the prices of the database (Column Cost €/m³). The total cost column refers to the sum of the construction costs of the complete frame, considering the total number of beams and columns. It should be pointed out that the price obtained has been estimated assuming that the model is constructed from zero. This is due to the fact that the aim of this study is to analyse the influence of the different constructive features in the ductility value, not its retrofitting. By considering the construction costs, it is possible to check whether the configuration that best improves the ductility and the performance of the building can be also competitive in terms of costs. The goal is to determine the most profitable solution taking into account other aspects rather than just the performance. The results obtained from this study can be applied in the design of new buildings and in the analysis of the ductility.

Table 6. Specific detail of the prices considering the characteristics of each of the models.

Models	Bay	Beams					Columns					Total Cost €	
		Wstirrups (kg)	Wrebar (kg)	Vconcrete (m ³)	Cost €/m ³	N° elements	Cost €	Wstirrups (kg)	Wrebar (kg)	Vconcrete (m ³)	Cost €/m ³		Cost €
Real	Exterior	12.78	104.15	1.13	282.29	6	1920.70	3.60	9.52	0.243	382.2	603.67	2908.5
	Interior	5.96	41.33	0.45	284.55	3	384.14						
RealMo	Exterior	12.78	104.15	1.13	340.18	6	2314.60	3.60	9.52	0.243	382.2	603.67	3380.50
	Interior	5.96	41.33	0.45	342.44	3	462.29						
M1	Exterior	10.66	129.92	0.75	376.03	6	1705.67	5.66	16.13	0.243	419.20	662.14	2708.90
	Interior	5.01	51.55	0.30	379.06	3	341.08						
H1	Exterior	19.28	89.49	1.51	267.86	6	2430.02	6.17	19.04	0.243	433.90	685.26	3600.95
	Interior	8.67	35.51	0.60	269.81	3	485.65						
M2	Exterior	16.18	111.87	1.13	293.37	6	1996.08	5.66	16.15	0.243	419.20	662.14	3058.56
	Interior	7.66	44.39	0.45	296.54	3	400.32						
H2	Exterior	19.16	130.38	1.13	314.85	6	2142.24	6.17	19.04	0.243	354.90	560.56	3132.43
	Interior	8.94	51.74	0.45	318.24	3	429.62						
S8	Exterior	22.65	104.15	1.13	292.12	6	1978.58	6.37	9.52	0.243	394.00	622.38	3009.69
	Interior	10.57	41.33	0.45	296.09	3	399.72						
S6_4LE	Exterior	17.13	108.01	1.13	290.54	6	1976.83	3.60	9.52	0.243	382.20	603.66	2976.69
	Interior	7.99	42.86	0.45	293.47	3	396.18						
Supduct	Exterior	25.55	104.15	1.13	295.05	6	2007.52	9.26	19.04	0.243	447.1	706.11	3116.56
	Interior	11.5	41.33	0.45	298.46	3	402.92						

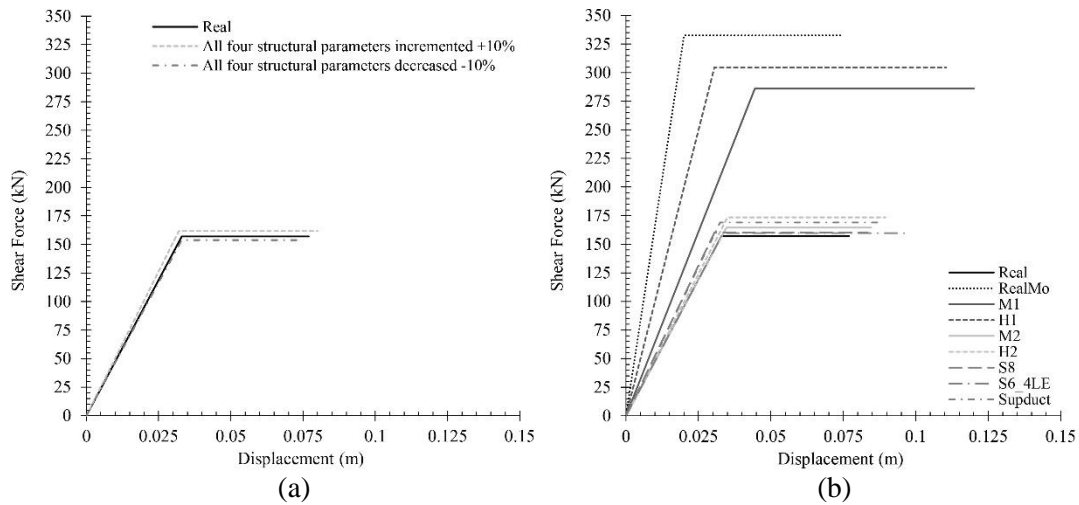
Regarding the damage level, a fragility curves approach has been followed according to (Estêvão 2019). Fragility curves provide the probability of reaching or exceeding a certain damage limit state (d_s) given a determined spectral acceleration ($a_{g,k}$), or the correspondent spectral displacement (S_d). The probability of occurrence of each damage limit state has been determined according to the fragility curves (obtained considering the building behaviour and (Estêvão 2019)) and the performance point (obtained according to the EC8-1 approach). Once the probability of reaching each damage limit has been determined, the mean damage index (DI) has been obtained according to the procedure established in (Vargas et al. 2013). This approach considers the three limit states defined in the EC8-3 (near collapse, significant damage and damage limitation) and the new one to be included in the future EC8 generation. This limit is called operability and it is included in the Italian Code NTC 2018 (Ministero delle infrastrutture e dei trasporti: Roma 2018).

There are numerous studies that proposed different DI approaches as in (Barbat et al. 2008). Unlike the rest of studies, the DI presented in (Vargas et al. 2013) is a very simple index which represents the total damage expected. It ranges between 0 and 4: DI=0 means that the probability of no-damage is equal to 1 while DI=4 indicates that a probability of complete damage state or collapse equals to 1. By calculating this DI, it is possible to compare the seismic performance of several models in terms of damage probability.

4. Results

The most relevant results obtained from the models analysed are shown in this section. In Fig. 7 (a), the idealized bilinear curves for the models considering the variability of the structural

518 parameters values are shown, while Fig. 7 (b) shows the idealized bilinear curves for each model
 519 considering the real values of the structural parameters.
 520



521
 522
 523 Fig. 7. Idealized bilinear curves for: (a) the models considering the variability of the structural
 524 parameters values and (b) the models in the X direction.
 525

526 Table 7 summarizes the μ -factor and the q -factor of all the models studied, highlighting the best
 527 q -factor results.
 528

529 Table 7. Nonlinear parameters of the models.

Models	Nonlinear parameters							
	Δ_u^* (m)	Δ_y^* (m)	μ	q_μ	V_y^* (kN)	V_d^* (kN)	q_Ω	q
Real	0.077	0.033	2.33	1.91	157.0	95.5	1.64	3.14
RealMo	0.075	0.020	3.75	2.54	332.5	178.5	1.86	4.74
M1	0.120	0.044	2.69	2.09	286.0	158.5	1.80	3.78
H1	0.110	0.030	3.62	2.49	304.5	155.0	1.96	4.90
M2	0.084	0.034	2.44	1.97	164.5	95.5	1.72	3.39
H2	0.089	0.035	2.55	2.02	173.5	95.0	1.82	3.7
S8	0.083	0.030	2.73	2.11	160.1	92.5	1.73	3.65
S6_4LE	0.096	0.033	2.86	2.17	159.8	91.5	1.74	3.79
Supduct	0.089	0.032	2.73	2.11	169.0	96.0	1.76	3.72

530
 531 In Table 8, the construction costs and the enhancement percentage of each solution are listed,
 532 respectively. Three percentages have been determined. The ratios represent the construction costs,
 533 μ -factor and q -factor of the assessed solution in relation to the existing buildings. The costs are
 534 presented in €/frame.
 535

536 Table 8. Construction costs and variation of costs, μ -factor and the q -factor with respect to the
 537 existing building and the ratio between the costs and the average μ - q .
 538

Models	Cost (€)	$C - C_{real} / C_{real}$ (%)	$\mu - \mu_{real} / \mu_{real}$ (%)	$q - q_{real} / q_{real}$ (%)	$Cost / Av (\mu \cdot q)$ €/%
Real	2908.51	-	-	-	-
RealMo	3380.55	16.23%	60.71%	50.86%	60.6
M1	2708.90	-6.86%	15.57%	20.14%	151.7
H1	3600.95	23.81%	55.27%	55.96%	64.7
M2	3058.56	5.16%	4.63%	7.82%	491.3
H2	3132.43	7.70%	9.59%	17.68%	229.7

S8	3009.69	3.48%	17.09%	16.17%	180.9
S6	2976.69	2.34%	22.81%	20.67%	136.9
Supduct	3116.56	7.15%	17.36%	18.32%	174.7

539

540

541

542

543

544

545

Based on the results of this phase, as discussed in the next section, the most relevant models (“Real” and “RealMo”) have been further analysed in order to obtain the global behaviour of the structures. In Table 9, the idealized bilinear curves parameters and the variation ratios of the two models are shown.

Table 9. Results for complete buildings.

Models	Δ_u^* (m)	Δ_y^* (m)	μ	V_y^* (kN)	V_d (kN)	q	C/C_{real} (%)	μ/μ_{real} (%)	q/q_{real} (%)
Real	0.105	0.041	2.56	1645.5	795.0	4.20	-	-	-
RealMo	0.108	0.028	3.88	1842.5	855.0	5.26	16.23%	35.74%	25.11%

546

547

548

549

Table 10 enlists the damage probability and the DI for each building model.

Table 10. Damage probability for each building.

Damage / Non damage Models	DI (%)	Slight D2 (%)	Moderate D3 (%)	Severe D4 (%)	Collapse D5 (%)	DI
Real	0	0.43	32.3	23.07	44.2	3.10
RealMo	0.21	3.25	62.63	20.8	13.23	2.43

550

551

552

553

5. Analysis of the results

554

555

556

557

558

559

The sensitivity analysis performed on the variability of the material properties suggests that the behaviour of the models studied barely depends on them. A maximum variation of a 3% in the idealized bilinear curves has been observed, for variations of up to +/-10% in the material properties. Therefore, this variability has been considered negligible and only the mean values have been used in the analyses.

560

561

562

563

564

565

566

567

568

569

570

571

572

573

For each of the constructive feature analysed, different results have been obtained. Concerning the geometrical properties, as can be observed in Fig. 7 (b), the deep-beam models (M1, H1 and RealMo) have outperformed the rest of the models. They have also presented the highest values of ductility, as shown in the last column of Table 7. However, H1 has been the most expensive solution due to the increase in the beams’ dimensions and reinforcement ratio. Models with wide beams (like the existing building) and enhanced reinforcement have merely shown a slight enhancement of the resistant capacity. The models designed with deep beams have presented higher variation ratios of μ -factor and q -factor as in (Gómez-Martínez et al. 2016b) and as shown in Table 7. Deep-beam models have reached up to 60% of ductility improvement compared to the existing building. Nevertheless, they have had the highest construction cost ratios (Table 8). This is due to the higher reinforcement ratios needed to comply with the code provisions and the beam’s volume. Still, the cost increase has been moderate (16% and 24%, respectively), especially considering the enhancements achieved.

574

575

576

577

578

579

580

581

Conversely, models where only the reinforcement ratios have been varied have presented relatively small variation ratios compared to deep-beam models. These enhancements have ranged from 5% to 10% in the case of the μ -factor and 8% to 18% for the q -factor. The construction cost ratios have been below 7%. The models with higher ratios (H2 and Supduct) have presented higher values of resisted shear forces. The S8 and the Supduct models have also enhanced their initial stiffness. The results obtained from the nonlinear static analyses have been similar to those in (Vielma et al. 2010), despite the different approach followed by the authors to define the bilinear curves. Similar results were obtained by (Lu et al. 2001) when assessing three

582 EC8-designed simple frames subjected to earthquake simulations. The authors concluded that the
583 amount of confining reinforcement at the critical regions of columns improved the local
584 behaviour. However, the overall ductility of frames was improved only slightly.

585
586 Yet, modifying the transversal reinforcement by adding four legged stirrups has caused a
587 considerable enhancement of the μ -factor and the q -factor up to 23% and 21%, respectively. This
588 is due to the reduction of the distance between consecutive longitudinal rebar engaged by stirrups.
589 This solution has presented almost no increase in costs compared to the existing building.

590
591 The ratio between the costs and the average μ - q have shown that the best models regarding the
592 costs are the RealMo and the H1. Contrariwise, the worst results have been obtained with the H2
593 and the S8 models. Based on these results, the RealMo model has been selected as the best
594 alternative to the existing building. This is due to the combination of the great improvement of
595 the μ -factor and q -factor, the simplicity and feasibility of the solution and its relatively low
596 increase in costs. The Real and RealMo models have been analysed considering all the bays of
597 the structure. The aim of these analyses is to study accurately the influence of varying the beam
598 orientations.

599
600 In the complete building analyses, the μ -factor and q -factor have been higher than the results
601 obtained for the single frame. This is due to the shear resistant capacity of the tie beams. The
602 damage level expected for the existing building has been severe ($DI>3$). Conversely, the RealMo
603 model has caused a reduction of the damage level of up to 28% compared to the existing building.
604 In this model, wide beams have been changed to deep beams, so this reduction can be further
605 improved by also increasing the reinforcement ratio.

606 607 608 **6. Conclusions**

609
610 This paper aims to analyse the ductility of existing buildings to evaluate its influence in their
611 seismic performance. This has been achieved through the retrospective analysis of an existing
612 building in accordance with current seismic codes.

613
614 The study has concluded that the NCSE02 and the EC8 share similar considerations concerning
615 the ductile capacity of new-designed buildings. However, each code establishes different
616 procedures and factors to determine this capacity i.e. μ -factor in the NCSE02 and q -factor in the
617 EC8, respectively. This study has revealed the lack of guidance in the NCSE02 and the EC8
618 regarding the assessment of the ductility of existing buildings. Although EC8-3 points out the
619 importance of analysing their seismic behaviour, no ductility considerations are taken into
620 account. This manuscript proposes a methodology to assess the ductility of Spanish existing
621 buildings.

622
623 In this study, a pushover analysis has been carried out first in one load-bearing frame of each of
624 nine different models. In these models, three different constructive features have been varied: the
625 beam dimensions (wide and deep beams), the longitudinal reinforcement and the transversal
626 reinforcement. The variability of the structural parameters has been analysed by modifying their
627 values. The results have not considerably differed from those considering the real values.
628 Therefore, this variability has been considered negligible and only the real structural values have
629 been used in the analyses carried out.

630
631 It can be concluded that the best performance, regarding the ductility, has been obtained with the
632 models designed with deep beams (RealMo and H1). It has also been demonstrated that these are
633 also the best models when considering the costs. Conversely, models with wide beams, and where
634 only the reinforcement ratios have been varied, have merely shown a slight enhancement of the
635 resistant capacity. Still, the models with higher reinforcement ratios have presented higher values
636 of resisted shear forces. Similarly, these models have shown relatively small improvements of μ -

637 factor and q -factor compared to deep-beam models. Yet, the addition of four legged stirrups has
638 brought a considerable enhancement of these factors. This is due to the reduction of the distance
639 between consecutive longitudinal rebar engaged by stirrups.

640

641 Based on the results of this first phase, the most relevant models have been analysed by means of
642 a similar pushover analysis, this time considering all the bays of the structure. The models
643 analysed have been the existing building and the model where only the orientation of the beams
644 has been changed (wide vs. deep beams). In these analyses, the μ -factor and q -factor have been
645 higher than the ones obtained for the single frame. This is due to the additional shear resistant
646 capacity of the tie beams. The expected damage has been severe for the existing building and
647 moderate for the deep beam model, respectively. Therefore, it can be concluded that, for a
648 minimum increase in cost, buildings using deep beams achieve an important enhancement in their
649 seismic behaviour.

650

651 This study has concluded that ductility affects the shear resistant capacity, and therefore, the
652 seismic performance and the expected damage of RC buildings. Hence, the ductility assessment
653 of these buildings must be performed thoroughly in order to propose appropriate seismic
654 retrofitting solutions.

655

656 **Acknowledgements**

657 This work has been supported by the INTERREG-POCTEP Spain-Portugal programme and the
658 European Regional Development Fund through the 0313_PERSISTAH_5_P project and the VI-
659 PPI of the University of Seville by the granting of a scholarship. The grant provided by the
660 Instituto Universitario de Arquitectura y Ciencias de la Construcción is acknowledged.

661

662 **References**

- 663 Abou-Elfath H, Elhout E (2018) Evaluating the Response Modification Factors of RC Frames
664 Designed with Different Geometric Configurations. *Int J Civ Eng* 16:1699-1711.
665 <https://doi.org/10.1007/s40999-018-0322-z>
- 666 Alam Shahria M, Moni M, Tesfamariam S (2012) Seismic overstrength and ductility of concrete
667 buildings reinforced with superelastic shape memory alloy rebar. *Eng Struct* 34:8-20.
668 <https://doi.org/10.1016/J.ENGSTRUCT.2011.08.030>
- 669 Alfarah B, López-Almansa F, Oller S (2017) New methodology for calculating damage
670 variables evolution in Plastic Damage Model for RC structures. *Eng Struct* 132:70-86.
671 <https://doi.org/10.1016/J.ENGSTRUCT.2016.11.022>
- 672 Amaro-Mellado JL, Morales-Esteban A, Martínez-Álvarez F (2017) Mapping of seismic
673 parameters of the Iberian Peninsula by means of a geographic information system. *Cent*
674 *Eur J Oper Res*. <https://doi.org/10.1007/s10100-017-0506-7>
- 675 Anagnostopoulou V V, Volakos EK, Zeris CA (2015) Objective evaluation of the q factor of
676 irregular RC buildings designed according to EC8-Design and analysis procedures. En: 5
677 th Conference on Computational Methods in Structural Dynamics and Earthquake
678 Engineering (ECCOMAS). Crete, pp 1040-1053
- 679 Applied Technology Council (ATC) (1998) FEMA 306: Evaluation of earthquake damaged
680 concrete and masonry wall buildings. US
- 681 Barbat AH, Pujades LG, Lantada N (2008) Seismic damage evaluation in urban areas using the
682 capacity spectrum method: Application to Barcelona. *Soil Dyn Earthq Eng* 28:851-865.
683 <https://doi.org/10.1016/j.soildyn.2007.10.006>
- 684 Calvi GM, Priestley MJN, Kowalsky MJ (2008) Displacement-based seismic design of
685 structures. En: 3rd National Conference on Seismic Engineering. Athens
- 686 Costa A, Romão X, Sousa Oliveira C, et al (2010) A methodology for the probabilistic
687 assessment of behaviour factors. *Bull Earthq Eng* 8:47-64. [https://doi.org/10.1007/s10518-](https://doi.org/10.1007/s10518-009-9126-5)
688 [009-9126-5](https://doi.org/10.1007/s10518-009-9126-5)
- 689 CYPE Ingenieros S.A. Construction costs database [Generador de precios]
- 690 Dassault Simulia (2014a) ABAQUS v6.14
- 691 Dassault Simulia (2014b) Abaqus/CAE User's Guide

692 Demir A, Caglar N, Ozturk H, Sumer Y (2016a) Nonlinear finite element study on the
693 improvement of shear capacity in reinforced concrete T-Section beams by an alternative
694 diagonal shear reinforcement. *Eng Struct* 120:158-165.
695 <https://doi.org/10.1016/J.ENGSTRUCT.2016.04.029>

696 Demir A, Caglar N, Ozturk H, Sumer Y (2016b) Nonlinear finite element study on the
697 improvement of shear capacity in reinforced concrete T-Section beams by an alternative
698 diagonal shear reinforcement. *Eng Struct* 120:158-165.
699 <https://doi.org/10.1016/J.ENGSTRUCT.2016.04.029>

700 Elnashai AS, Mwafy AM (2002) Overstrength and force reduction factors of multistorey
701 reinforced-concrete buildings. *Struct Des Tall Build* 11:329-351.
702 <https://doi.org/10.1002/tal.204>

703 Estêvão JMC (2019) An integrated computational approach for seismic risk assessment of
704 individual buildings. *Appl Sci* 9:. <https://doi.org/10.3390/app9235088>

705 European Union (2005) Eurocode-8: Design of structures for earthquake resistance. Part 3:
706 Assessment and retrofitting of buildings. Belgium

707 European Union (2004a) Eurocode 8: Design of structures for earthquake resistance. Part 1:
708 General rules, seismic actions and rules for buildings. Belgium

709 European Union (2004b) Eurocode-2: Design of concrete structures. Part 1-1: General rules and
710 rules for buildings. Brussels

711 Fajfar P (1999) Capacity spectrum method based on inelastic demand spectra. *Earthq Eng Struct*
712 *Dyn* 28:979-993. https://doi.org/10.1007/978-3-642-36197-5_201-1

713 Fajfar P (2000) A nonlinear analysis method for performance-based seismic design. *Earthq*
714 *Spectra* 16:573-592. <https://doi.org/https://doi.org/10.1193/1.1586128>

715 Ferraioli M, Lavino A, Mandara A (2014) Behaviour factor of code-designed steel moment-
716 resisting frames. *Int J Steel Struct* 14:243-254. <https://doi.org/10.1007/s13296-014-2005-1>

717 Fu F (2009) Progressive collapse analysis of high-rise building with 3-D finite element
718 modeling method. *J Constr Steel Res* 65:1269-1278.
719 <https://doi.org/10.1016/J.JCSR.2009.02.001>

720 Gómez-Martínez F, Alonso-Durá A, De Luca F, Verderame GM (2016a) Seismic performances
721 and behaviour factor of wide-beam and deep-beam RC frames. *Eng Struct* 125:107-123.
722 <https://doi.org/10.1016/J.ENGSTRUCT.2016.06.034>

723 Gómez-Martínez F, Alonso-Durá A, De Luca F, Verderame GM (2016b) Seismic performances
724 and behaviour factor of wide-beam and deep-beam RC frames. *Eng Struct* 125:107-123.
725 <https://doi.org/10.1016/J.ENGSTRUCT.2016.06.034>

726 Grassl P, Xenos D, Nyström U, et al (2013) CDPM2: A damage-plasticity approach to
727 modelling the failure of concrete. *Int J Solids Struct* 50:3805-3816.
728 <https://doi.org/10.1016/J.IJSOLSTR.2013.07.008>

729 Kappos A. (1999) Evaluation of behaviour factors on the basis of ductility and overstrength
730 studies. *Eng Struct* 21:823-835. [https://doi.org/10.1016/S0141-0296\(98\)00050-9](https://doi.org/10.1016/S0141-0296(98)00050-9)

731 Khose VN, Singh Y, Lang DH (2012) A comparative study of design base shear for RC
732 buildings in selected seismic design codes. *Earthq Spectra* 28:1047-1070.
733 <https://doi.org/10.1193/1.4000057>

734 Lee J, Fenves GL (1998) Plastic-damage model for cyclic loading of concrete structures. *J Eng*
735 *Mech* 124:892-900. [https://doi.org/10.1061/\(ASCE\)0733-9399\(1998\)124:8\(892\)](https://doi.org/10.1061/(ASCE)0733-9399(1998)124:8(892))

736 Lu Y, Hao H, Carydis P., Mouzakis H (2001) Seismic performance of RC frames designed for
737 three different ductility levels. *Eng Struct* 23:537-547. [https://doi.org/10.1016/S0141-](https://doi.org/10.1016/S0141-0296(00)00058-4)
738 [0296\(00\)00058-4](https://doi.org/10.1016/S0141-0296(00)00058-4)

739 Lubliner J, Oliver J, Oller S, Onate E (1989) A plastic-damage model for concrete. *Int J Solids*
740 *Struct* 25:299-326. [https://doi.org/10.1016/0020-7683\(89\)90050-4](https://doi.org/10.1016/0020-7683(89)90050-4)

741 Manfredi V, Masi A (2017) Consistency of analysis methods considered in EC8-3 for the
742 seismic assessment of RC existing buildings. *Bull Earthq Eng* 15:3027-3051.
743 <https://doi.org/10.1007/s10518-016-0070-x>

744 Ministero delle infrastrutture e dei trasporti: Roma (2018) NTC. Aggiornamento delle «Norme
745 tecniche per le costruzioni». Italy

746 Miranda E, Bertero V V. (1994) Evaluation of strength reduction factors for earthquake-

747 resistant design. *Earthq Spectra* 10:357-379. <https://doi.org/10.1193/1.1585778>

748 Mondal A, Ghosh S, Reddy GR (2013) Performance-based evaluation of the response reduction
749 factor for ductile RC frames. *Eng Struct* 56:1808-1819.
750 <https://doi.org/10.1016/J.ENGSTRUCT.2013.07.038>

751 Mwafy AM, Elnashai AS, Elnashai' AS (2002) Calibration of force reduction factors of RC
752 buildings. *J Earthq Eng ISSN* 6:234-273. <https://doi.org/10.1080/13632460209350416>

753 O'Reilly GJ, Perrone D, Fox M, et al (2018) Seismic assessment and loss estimation of existing
754 school buildings in Italy. *Eng Struct* 168:142-162.
755 <https://doi.org/10.1016/j.engstruct.2018.04.056>

756 O'Reilly GJ, Sullivan TJ (2018) Probabilistic seismic assessment and retrofit considerations for
757 Italian RC frame buildings. Springer Netherlands

758 Park R (1998) State-of-the-art report: ductility evaluation from laboratory and analytical testing.
759 En: *Proceedings of 9th World Conference on Earthquake Engineering*. Kyoto, pp 605–616

760 Requena-García-Cruz MV, Morales-Esteban A, Durand-Neyra P, Estêvão JMC (2019) An
761 index-based method for evaluating seismic retrofitting techniques. Application to a
762 reinforced concrete primary school in Huelva. *PLoS One* 14:e0215120.
763 <https://doi.org/10.1371/journal.pone.0215120>

764 Reza Azadi Kakavand M, Neuner M, Schreter M, Hofstetter G (2018) A 3D continuum FE-
765 model for predicting the nonlinear response and failure modes of RC frames in pushover
766 analyses. *Bull Earthq Eng* 16:4893-4917. <https://doi.org/10.1007/s10518-018-0388-7>

767 Rodgers J (2012) Why schools are vulnerable to earthquakes. *15th World Conf Earthq Eng*

768 Sá L, Morales-Esteban A, Durand Neyra P (2018) The 1531 earthquake revisited : loss
769 estimation in a historical perspective. *Bull Earthq Eng* 16:4533-4559.
770 <https://doi.org/10.1007/s10518-018-0367-z>

771 Spanish Ministry of Public Works [Ministerio de Fomento de España] (2002) Spanish Seismic
772 Construction Code of Buildings [Norma de Construcción Sismorresistente: Parte general y
773 edificación (NSCE-02)]. Spain

774 Spanish Ministry of Public Works [Ministerio de Fomento de España] (2008) Structural
775 concrete code [Instrucción de Hormigón Estructural (EHE-08)]

776 Spanish Ministry of Public Works [Ministerio de Fomento de España] (1994) Spanish seismic
777 code 1994 (NCSE94)

778 Spanish Ministry of Public Works [Ministerio de Fomento de España] (2012) Update of the
779 seismic hazard maps [Actualización de mapas de peligrosidad sísmica de España]. Spain

780 Spanish Ministry of Public Works [Ministerio de Fomento de España] (1998) Spanish annex to
781 Eurocode-8 [Anexo español al Eurocódigo 8]. Madrid

782 Spanish Ministry of Public Works [Ministerio de Fomento de España] (2009) Structural
783 security: actions in buildings [Seguridad Estructural Acciones en la edificación (CTE-DB-
784 SE-AE)]

785 Taieb B, Sofiane B (2014) Accounting for ductility and overstrength in seismic design of
786 reinforced concrete structures. *Proc 9th Int Conf Struct Dyn (EURODYN 2014)* 311-314

787 Tao Y, Chen J f (2015) Concrete Damage Plasticity Model for modeling FRP-to-concrete bond
788 behavior. *J Compos Constr* 19:1-13. [https://doi.org/10.1061/\(ASCE\)CC.1943-5614.0000482](https://doi.org/10.1061/(ASCE)CC.1943-5614.0000482)

789

790 Vargas YF, Pujades LG, Barbat AH, Hurtado JE (2013) Capacity, fragility and damage in
791 reinforced concrete buildings: A probabilistic approach. *Bull Earthq Eng* 11:2007-2032.
792 <https://doi.org/10.1007/s10518-013-9468-x>

793 Vielma JC, Barbat AH, Oller S (2010) Seismic safety of low ductility structures used in Spain.
794 *Bull Earthq Eng* 8:135-155. <https://doi.org/10.1007/s10518-009-9127-4>

795 Vona M, Mastroberti M (2018) Estimation of the behavior factor of existing RC-MRF
796 buildings. *Earthq Eng Vib* 17:191-204. <https://doi.org/10.1007/s11803-018-0434-0>

797 Zahid MZAM, Robert D, Shahrin F (2013) An evaluation of overstrength factor of seismic
798 designed low rise RC buildings. *Procedia Eng* 53:48-51.
799 <https://doi.org/10.1016/j.proeng.2013.02.008>

800 Zerbin M, Aprile A, Beyer K, Spacone E (2019) Ductility reduction factor formulations for
801 seismic design of RC wall and frame structures. *Eng Struct* 178:102-115.

802 <https://doi.org/10.1016/J.ENGSTRUCT.2018.10.020>
803 Žižmond J, Dolšek M (2016) Evaluation of factors influencing the earthquake-resistant design
804 of reinforced concrete frames according to Eurocode 8. Struct Infrastruct Eng 12:1323-
805 1341. <https://doi.org/10.1080/15732479.2015.1117112>
806